Extracting the angle of release from guitar tones: preliminary results

Bertrand Scherrer, Philippe Depalle

ACOUSTICS 2012

Extracting the angle of release from guitar tones: preliminary results

B. Scherrer and P. Depalle

McGill University, CIRMMT, SPCL, Schulich School of Music, 555 Sherbrooke Street West, Montréal, Canada H3A1E3
bertrand.scherrer@mail.mcgill.ca

On the classical guitar, a performer can impart very distinct qualities upon the sound s/he produces by the way s/he plucks the strings. There is, for example, a clearly audible difference between notes plucked using a rest stroke (or "buté") and a free stroke (or "tiré"). The difference between these strokes has been shown to stem from a difference in the angle at which the string is released at the end of the finger-string interaction. A sound analysis tool, based on a digital waveguide model that exploits the asymmetry of the guitar body's admittance, has been created to provide an estimate of this angle of release. Some first results on synthetic signals are presented. This work is an extension of a previous study in which the plucking position was extracted from an audio recording.

1 Introduction

Guitarists have many playing techniques they can resort to control the timbre of a given pluck (see [9] for examples). Most of these technique affect the initial conditions of the free oscillation of the string, at the end of the finger-string interaction.

In this paper, the focus is on one parameter of the plucking action: the angle with which the string is released at the end of the finger-string interaction. While most guitarists may not be familiar with the angle of release (θ_r) per se, they change it when choosing between a rest stroke (where the plucking finger rests on the next string) and a free stroke (where the plucking finger clears the next string). The plot on the right of Fig. 1, shows the difference in θ_r between a free stroke and a rest stroke, respectively, as measured by [7]. The circled dots marked l_{free} and l_{rest} represent the points at which the string is released from the finger for the free stroke and the rest stroke, respectively.

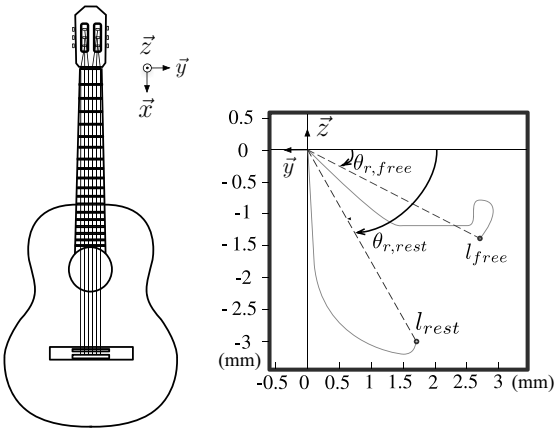

Figure 1: Coordinate system used in this paper (left), and measured trajectories of the string, near the plucking point, for rest and free strokes adapted from [7] (right).

In the following, a physically-informed signal analysis technique is presented. Its aim is to determine how a guitar was played from the analysis of a recording of the velocity at the bridge. A similar, approach was used in [13] where the plucking position on a string was extracted from the analysis of a sound recording. In [13], as is the case here, the modelling of the effect of a particular plucking gesture on the sound is central to the estimation method.

The model presented in Sec. 2 makes the influence of θ_r on the velocity at the bridge explicit. Then, the strategy used to estimate the angle of release from structural modal parameters is derived in Sec. 3. Sec. 4 presents the complete analysis framework used to retrieve θ_r starting from the extraction of modal parameters of a given bridge velocity signal. Finally, the performance of the strategy as currently implemented is evaluated on synthetic velocity signals in Sec. 5.

2 Modelling the plucking gestures

The Digital Waveguide (DW) paradigm [10][1] is used to devise a model for the vibration of one guitar string that takes into account both the plucking position and θ_r. More specifically, a string is represented by two bi-directional delay lines: the "normal" ($\vec{z}$ in Fig. 1) and "parallel" ($\vec{y}$ in Fig. 1) directions[2]. The torsional and longitudinal modes of vibration are not taken into account in this study. The coupling occurring between the two transverse directions at the bridge is modelled using reflectance functions [10][3] as shown in Fig. 2.

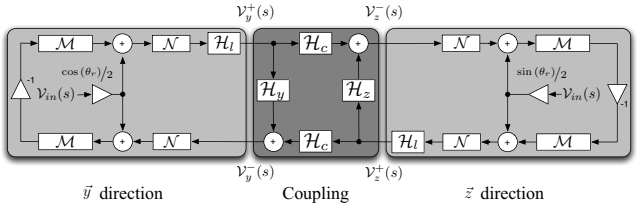

Figure 2: Diagram of the DW network simulating a string observed along the y and z directions, including the coupling at the bridge. The Laplace variable is denoted 's'.

The angle, θ_r, distributes the input velocity, $\mathcal{V}_{in}(s)$, between the two transverse directions. The losses occurring during a round trip around the string, as well as the potential stiffness of the string, are modelled using the filter $\mathcal{H}_l(s)$. The terms of the 2×2 admittance matrix at the bridge, as well as the characteristic impedance of the string are encapsulated in the reflectances $\mathcal{H}_y(s)$, $\mathcal{H}_z(s)$, and $\mathcal{H}_c(s)$. Finally, the propagation of the waves from the plucking point to the bridge, and from the plucking point to the nut (or fret), are modelled using pure delay lines of lengths $\mathcal{N}$ and $\mathcal{M}$, respectively.

Since, the ultimate goal of this work is to estimate θ_r from the analysis of the sound of a guitar captured by a microphone, it is important to consider the radiation pattern of the instrument. From the results found in [4], it is assumed that the sound radiated by a guitar, directly in front of it, mostly depends on the displacement of the bridge along the $\vec{z}$ direction (cf. Fig. 1). This is why we focus our attention on the transfer function, $\mathcal{T}_z$, of the $\vec{z}$ direction[4]:

$$\mathcal{T}_z = \frac{\mathcal{V}_z}{\mathcal{V}_{ex}} = \frac{\gamma + \zeta e^{-\mathcal{D}s}}{1 + \alpha e^{-\mathcal{D}s} + \beta e^{-2\mathcal{D}s}} \tag{1}$$

where:

$$\begin{aligned} \mathcal{D} &= 2\mathcal{M} + 2\mathcal{N} \\ \mathcal{V}_{ex} &= \frac{\mathcal{V}_{in}}{2}\mathcal{H}_l e^{-\mathcal{N}s}\left(1 - e^{-2\mathcal{M}s}\right) \end{aligned}$$

[1] https://ccrma.stanford.edu/~jos/pasp/, accessed March 9, 2012.

[2] with respect to the top plate of the guitar.

[3] https://ccrma.stanford.edu/~jos/pasp/Bridge_Reflectance.html, accessed March 9, 2012.

[4] From now on, we omit the Laplace variable "s", when it is not required.

$$\begin{aligned}\alpha &= \mathcal{H}_l\left[\mathcal{H}_y + \mathcal{H}_z\right]\\ \beta &= \mathcal{H}_l^2\left[\mathcal{H}_y\mathcal{H}_z - \mathcal{H}_c^2\right]\\ \gamma &= \left[1+\mathcal{H}_z\right]\sin(\theta_r) + \mathcal{H}_c\cos(\theta_r)\\ \zeta &= \mathcal{H}_l\left[(1+\mathcal{H}_z)\mathcal{H}_y - \mathcal{H}_c^2\right]\sin(\theta_r)\\ &\quad -\mathcal{H}_c H_l\cos(\theta_r)\end{aligned}$$

A few observations can be made based on the expression of $\mathcal{T}_z$:

- θ_r is present at the numerator of $\mathcal{T}_z$; this means that θ_r will influence the amplitudes and phases of the frequency components forming a partial.
- as expected, due to the coupling, the denominator of $\mathcal{T}_z$ will exhibit two groups of poles occurring at neighbouring frequencies. One such pair of poles, when analyzed using Fourier analysis, will give rise to one partial with a potentially beating amplitude envelope.

3 Estimating the Angle of Release

The approach used to estimate θ_r is adapted from studies of the coupling between strings [1] and between polarizations of a same string [3] on the piano.

Here, it is the velocity of the string at the bridge, captured by an accelerometer that is the starting point of the analysis. The admittance terms have also been measured as in [14], and modelled as in [2]. This is slightly different from [3], and [1], where the transverse displacements along two orthogonal directions of one string, and the vertical displacements of two separate strings were measured, respectively, as the input of the analysis procedure.

It follows from Eq. (1) that the velocity signal, $\mathcal{V}_z$, recorded by the accelerometer placed on the bridge saddle has a spectrum of the form:

$$\mathcal{V}_z(\omega) = \sum_k \underbrace{\frac{g_{1k}}{\delta_{1k}+i(\omega-\omega_{1k})} + \frac{g_{2k}}{\delta_{2k}+i(\omega-\omega_{2k})}}_{\mathcal{V}_{zk}(\omega)} \text{ for } \omega \geq 0 \tag{2}$$

where ω_{1k}, δ_{1k}, g_{1k} and ω_{2k}, δ_{2k}, g_{2k} are the radian frequencies, damping factors and complex amplitudes of the two components forming the k^{th} "partial": $\mathcal{V}_{zk}(\omega)$.

3.1 Relating the signal parameters to the elements of the model

By comparing the expressions of $\mathcal{T}_z(\omega)\mathcal{V}_{ex}(\omega)$ and $\mathcal{V}_z(\omega)$ around the frequencies of the partials, one can obtain the expressions of g_{1k}, g_{2k}, δ_{1k}, δ_{2k}, ω_{1k}, ω_{2k} as functions of θ_r, $\mathcal{H}_y$, $\mathcal{H}_z$, $\mathcal{H}_c$, $\mathcal{H}_l$ and $\mathcal{D}$.

First, we perform a partial fraction expansion of $\mathcal{T}_z$, introducing the intermediary terms $\mathcal{P}(\omega)$, $\mathcal{Q}(\omega)$, $\mathcal{A}(\omega)$ and $\mathcal{B}(\omega)$[5]:

$$\begin{aligned}\mathcal{T}_z &= \frac{\mathcal{P}}{1-\mathcal{A}e^{-i\omega\mathcal{D}}} + \frac{\mathcal{Q}}{1-\mathcal{B}e^{-i\omega\mathcal{D}}}\\ &= \frac{[\mathcal{P}+\mathcal{Q}] - [\mathcal{P}\mathcal{B}+\mathcal{Q}\mathcal{A}]\,e^{-i\omega\mathcal{D}}}{1-[\mathcal{A}+\mathcal{B}]\,e^{-i\omega\mathcal{D}} + \mathcal{A}\mathcal{B}e^{-i2\omega\mathcal{D}}}\end{aligned} \tag{3}$$

[5] the variable ω will be omitted for readability.

Comparing Eq. (1) and Eq. (3), with $s = i\omega$:

$$\mathcal{P}+\mathcal{Q} = \left[1+\mathcal{H}_z\right]\sin(\theta_r) + \mathcal{H}_c\cos(\theta_r) \tag{4}$$

$$\begin{aligned}\mathcal{P}\mathcal{B}+\mathcal{Q}\mathcal{A} &= \mathcal{H}_l\left[\mathcal{H}_c^2 - (1+\mathcal{H}_z)\mathcal{H}_y\right]\sin(\theta_r)\\ &\quad +\mathcal{H}_c\mathcal{H}_l\cos(\theta_r)\end{aligned} \tag{5}$$

$$\mathcal{A}+\mathcal{B} = -\mathcal{H}_l\left[\mathcal{H}_y+\mathcal{H}_z\right] \tag{6}$$

$$\mathcal{A}\mathcal{B} = \mathcal{H}_l^2\left[\mathcal{H}_y\mathcal{H}_z - \mathcal{H}_c^2\right] \tag{7}$$

For ω in the direct vicinity of partial k, considering that string partials do not overlap in frequency[6], we can write:

$$\mathcal{V}_z(\omega) \simeq \mathcal{V}_{zk}(\omega) = \frac{g_{1k}}{\delta_{1k}+i(\omega-\omega_{1k})} + \frac{g_{2k}}{\delta_{2k}+i(\omega-\omega_{2k})} \tag{8}$$

Identifying $\mathcal{V}_z$ and $\mathcal{T}_z\mathcal{V}_{ex}$ around partial k we get:

$$\begin{aligned}\frac{\mathcal{P}\mathcal{V}_{ex}}{1-\mathcal{A}e^{-i\omega\mathcal{D}}} + \frac{\mathcal{Q}\mathcal{V}_{ex}}{1-\mathcal{B}e^{-i\omega\mathcal{D}}} &\simeq \frac{g_{1k}}{\delta_{1k}+i(\omega-\omega_{1k})}\\ &\quad + \frac{g_{2k}}{\delta_{2k}+i(\omega-\omega_{2k})}\end{aligned} \tag{9}$$

If we consider that component 1 (right of "$\simeq$") corresponds to the term with denominator $1-\mathcal{A}e^{-i\omega\mathcal{D}}$ (left of "$\simeq$"), we can derive the expression for ω_{1k}:

$$\omega_{1k} = \frac{\Phi_A(\omega_{1k}) + k2\pi}{\mathcal{D}} \tag{10}$$

To determine the expressions of g_{1k} and δ_{1k}, we consider the frequency range $\omega = \omega_{1k} + \epsilon$ with:

$$\epsilon << \min_k(|\omega_{1k} - \omega_{2k}|)$$

In that frequency range, we can write:

$$\begin{aligned}\frac{G(\omega_{1k}+\epsilon)}{1-F(\omega_{1k}+\epsilon)} &= \frac{g_{1k}}{\delta_{1k}+i\epsilon}\\ \text{where } G(\omega) &= \mathcal{P}(\omega)\mathcal{V}_{ex}(\omega)\\ F(\omega) &= \rho_{\mathcal{A}}(\omega)e^{i(\Phi_{\mathcal{A}}(\omega)-\omega\mathcal{D})}\end{aligned} \tag{11}$$

By taking a Taylor series expansions at the 0^{th} order for the numerator, and at the 1^{st} order for the denominator one gets:

$$\begin{aligned}\frac{G(\omega_{1k}+\epsilon)}{1-F(\omega_{1k}+\epsilon)} &\simeq \frac{G(\omega_{1k})}{1-(F(\omega_{1k})+\epsilon F'(\omega_{1k}))}\\ \text{with } F'(\omega) &= \left(\rho'_{\mathcal{A}}(\omega) + i\left(\Phi'_{\mathcal{A}}(\omega)-\mathcal{D}\right)\right)F(\omega)\end{aligned}$$

Using Eq. (10), we can write:

$$F(\omega_{1k}) = |\mathcal{A}(\omega_{1k})|$$

If we assume that $\rho'_{\mathcal{A}} \simeq 0$ and that $\Phi'_{\mathcal{A}}(\omega_{1k}) << \mathcal{D}$[7], we can use Eq. (11) to identify the coefficients of ϵ on both sides of the $\simeq$ sign:

$$g_{1k} \simeq \frac{\mathcal{P}(\omega_{1k})\mathcal{V}_{ex}(\omega_{1k})}{|\mathcal{A}(\omega_{1k})|\mathcal{D}} \tag{12}$$

$$\delta_{1k} \simeq \frac{1-|\mathcal{A}(\omega_{1k})|}{|\mathcal{A}(\omega_{1k})|\mathcal{D}} \tag{13}$$

[6] reasonable assumptions when the lowest note on a classical guitar, using normal tuning, has a frequency of $\simeq 82$ Hz and a decay factor of $\simeq 2\,s^{-1}$; this means that partial k contributes $\simeq -60$ dB to the power of partial $k+1$.

[7] verified experimentally.

A similar procedure allows to retrieve the parameters of the second component:

$$\omega_{2k} = \frac{\Phi_{\mathcal{B}}(\omega_{2k}) + k2\pi}{\mathcal{D}} \quad (14)$$

$$g_{2k} \simeq \frac{\mathcal{Q}(\omega_{2k})\mathcal{V}_{ex}(\omega_{2k})}{|\mathcal{B}(\omega_{2k})|\mathcal{D}} \quad (15)$$

$$\delta_{2k} \simeq \frac{1 - |\mathcal{B}(\omega_{2k})|}{|\mathcal{B}(\omega_{2k})|\mathcal{D}} \quad (16)$$

3.2 Expression of θ_r

From the expressions established in Sec. 3.1, one can revert the process and estimate θ_r from the estimation of the parameters of $S_z(\omega)$. The analysis framework used to retrieve these parameters is detailed in Sec. 4.

Here are the steps necessary to obtain the expression of θ_r:

1. With the measurement of the fundamental frequency of the signal, $\hat{f}_0$, the delay, $\mathcal{D}$, in seconds, can be estimated as:
$$\hat{\mathcal{D}} = \frac{1}{\hat{f}_0}$$

2. From the estimation of the pulsations and damping factors of the two components ($\hat{\omega}_{1k}$, $\hat{\omega}_{2k}$, $\hat{\delta}_{1k}$, and $\hat{\delta}_{2k}$) the values of $\mathcal{A}$ and $\mathcal{B}$ around the pulsations of the k^{th} partial of both components can be found. To do this, one needs to assume that:
$$\begin{aligned}\mathcal{A}(\omega_{1k}) &\simeq \mathcal{A}(\omega_{2k}) \triangleq \mathcal{A}_k\\ \mathcal{B}(\omega_{1k}) &\simeq \mathcal{B}(\omega_{2k}) \triangleq \mathcal{B}_k\end{aligned}$$
From Eqs. (13) and (16) as well as from Eqs. (10) and (14) one then finds:
$$\hat{\mathcal{A}}_k = \left|\hat{\mathcal{A}}_k\right| e^{i\hat{\Phi}_{\hat{\mathcal{A}}_k}} = \frac{e^{i\hat{\mathcal{D}}\hat{\omega}_{1k}}}{\hat{\delta}_{1k}\hat{\mathcal{D}} + 1} \quad (17)$$
$$\hat{\mathcal{B}}_k = \left|\hat{\mathcal{B}}_k\right| e^{i\hat{\Phi}_{\hat{\mathcal{B}}_k}} = \frac{e^{i\hat{\mathcal{D}}\hat{\omega}_{2k}}}{\hat{\delta}_{2k}\hat{\mathcal{D}} + 1} \quad (18)$$

3. In a way similar to what we just did for $\mathcal{A}$ and $\mathcal{B}$, we define $\mathcal{H}_{y,k}$, $\mathcal{H}_{z,k}$. These values can be computed from the admittance term measurements and, using Eq. (6), one can get the following expression of $\hat{\mathcal{H}}_{l,k}$:
$$\hat{\mathcal{H}}_{l,k} = -\frac{\hat{\mathcal{A}}_k + \hat{\mathcal{B}}_k}{\hat{\mathcal{H}}_{y,k} + \hat{\mathcal{H}}_{z,k}} \quad (19)$$

4. Defining:
$$\eta(\omega) = \frac{\mathcal{P}(\omega)}{\mathcal{Q}(\omega)}$$
for any ω, one can write Eqs. (4) and (5) as:
$$\begin{aligned}\mathcal{P} + \mathcal{Q} &= \mathcal{Q}(\eta + 1)\\ \mathcal{P}\mathcal{B} + \mathcal{Q}\mathcal{A} &= \mathcal{Q}(\eta\mathcal{B} + \mathcal{A})\end{aligned}$$

5. Let us now define Ψ as the ratio between the right hand sides of Eqs. (4) and (5):
$$\begin{aligned}\Psi &= \frac{\eta + 1}{\mathcal{B}\eta + \mathcal{A}}\\ &= \frac{(1 + \mathcal{H}_z)\tan(\theta_r) + \mathcal{H}_c}{\mathcal{H}_l\left[\mathcal{H}_c^2 - (1 + \mathcal{H}_z)\mathcal{H}_y\right]\tan(\theta_r) + \mathcal{H}_l\mathcal{H}_c} \quad (20)\end{aligned}$$

From Eq. (12) and Eq. (15), assuming that:

$$\begin{aligned}\mathcal{P}(\omega_{1k}) &\simeq \mathcal{P}(\omega_{2k}) = \mathcal{P}_k\\ \mathcal{Q}(\omega_{1k}) &\simeq \mathcal{Q}(\omega_{2k}) = \mathcal{Q}_k\\ \mathcal{V}_{ex}(\omega_{1k}) &\simeq \mathcal{V}_{ex}(\omega_{2k}) = \mathcal{V}_{ex,k}\end{aligned}$$

we have:
$$\eta_k = \frac{\hat{g}_{1k}|\hat{\mathcal{A}}_k|}{\hat{g}_{2k}|\hat{\mathcal{B}}_k|} \quad (21)$$

Finally, from Eq. (21) and (20) we can write:

$$\tan(\theta_r) = \frac{C_{1k}\frac{\hat{g}_{1k}}{\hat{g}_{2k}} + C_{2k}}{C_{3k}\frac{\hat{g}_{1k}}{\hat{g}_{2k}} + C_{4k}} \quad (22)$$

where :

$$\begin{aligned}C_{1k} &= |\hat{\mathcal{A}}_k|\hat{\mathcal{H}}_{c,k}\left(\hat{\mathcal{B}}_k - \hat{\mathcal{H}}_{l,k}\right)\\ C_{2k} &= |\hat{\mathcal{B}}_k|\hat{\mathcal{H}}_{c,k}\left(\hat{\mathcal{A}}_k - \hat{\mathcal{H}}_{l,k}\right)\\ C_{3k} &= |\hat{\mathcal{A}}_k|\left(\hat{\mathcal{H}}_{l,k}\hat{\mathcal{H}}_{c,k}^2 - \left(1 + \hat{\mathcal{H}}_{z,k}\right)\left(\hat{\mathcal{B}}_k + \hat{\mathcal{H}}_{l,k}\hat{\mathcal{H}}_{y,k}\right)\right)\\ C_{4k} &= |\hat{\mathcal{B}}_k|\left(\hat{\mathcal{H}}_{l,k}\hat{\mathcal{H}}_{c,k}^2 - \left(1 + \hat{\mathcal{H}}_{z,k}\right)\left(\hat{\mathcal{A}}_k + \hat{\mathcal{H}}_{l,k}\hat{\mathcal{H}}_{y,k}\right)\right)\end{aligned}$$

This final equation provides the expression of the angle of release as a function of parameters that can be estimated from the analysis of the measured velocity signal as well as from some admittance measurements.

We can further simplify the expressions of the $C_{i,k}$ coefficients using the measured admittance data. Indeed, a first approximation that appears from observing simulated $A(\omega)$ and $B(\omega)$, allows us to write:

$$\begin{aligned}\mathcal{A}(\omega) &\simeq -\mathcal{H}_l(\omega)\mathcal{H}_z(\omega)\\ \mathcal{B}(\omega) &\simeq -\mathcal{H}_l(\omega)\mathcal{H}_y(\omega)\end{aligned}$$

Indeed, the ratios $\mathcal{A}/\mathcal{H}_l\mathcal{H}_z$ and $\mathcal{B}/\mathcal{H}_l\mathcal{H}_z$ were measured as being very close to 1 for most frequencies (with a maximum error of 2%). We also noticed that $C_{4,k}$ remained unchanged when computed with or without the term in $\mathcal{H}_c^2$. On the other hand, we also observed that, if the term in $\mathcal{H}_c^2$ was omitted, $C_{3,k}$ was affected more significantly. This allows us to define a set of approximate coefficients:

$$\tilde{C}_{1k} = -\mathcal{H}_{c,k}|\mathcal{H}_{z,k}|(1 + \mathcal{H}_{y,k}) \quad (23)$$

$$\tilde{C}_{2k} = -\mathcal{H}_{c,k}|\mathcal{H}_{y,k}|(1 + \mathcal{H}_{z,k}) \quad (24)$$

$$\tilde{C}_{3,k} = |\mathcal{H}_{z,k}|\left[\mathcal{H}_{c,k}^2 - (1 + \mathcal{H}_{z,k})\left(\mathcal{B}_k/\mathcal{H}_{l,k} + \mathcal{H}_{y,k}\right)\right] \quad (25)$$

$$\tilde{C}_{4,k} = -|\mathcal{H}_{y,k}|(1 + \mathcal{H}_{z,k})\left(\mathcal{H}_{y,k} - \mathcal{H}_{z,k}\right) \quad (26)$$

4 Analysis Framework

The analysis framework presented in this section aims at extracting the signal parameters necessary to estimate θ_r following the method presented in Sec. 3.2.

The first step in the analysis chain is to pre-process the sound (high-pass filtering, DC-removal). Then, after detecting the percussive onset(s), the signal is segmented into individual plucks, and the steady-state portion of these plucks are selected for analysis. In a global analysis step, the fundamental frequency is estimated on the audio segment. Then, a standard additive analysis is carried out (e.g. [11]) to identify the string partials. The frequency resolution provided by this

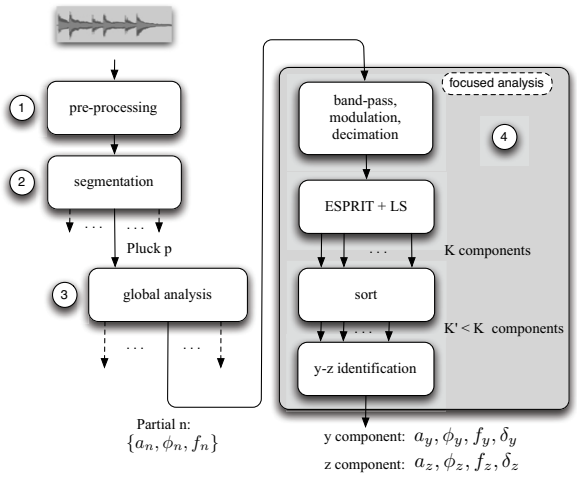

Figure 3: Analysis framework to extract the signal parameters required to determine θ_r from a velocity measurement.

analysis step is not sufficient, however, for the task of determining the frequency, damping factor, amplitude, and phase of the closely coupled modes in a given string partial.

Hence, the next step of the analysis chain consists of a focused analysis around each string partial. The frequencies and damping factors of the modes are estimated using the ESPRIT method [8]. The amplitudes and initial phases of the poles are estimated via the least squares method. To avoid numerical issues, a multi-band approach is adopted along with under-sampling [5]. In other words, ESPRIT looks for K exponentially decaying sinusoids around each partial. The partials are isolated using a near-linear phase filter of the type of those presented in [6]. The resulting signal is then under-sampled.

Based on the model in Sec. 2, $K = 2$ should suffice since we assume a string partial is the result of the coupling of two transverse directions only. With ESPRIT, as with such parametric methods however, an overestimated K is often advisable ($K = 3$ in practice). Therefore, a pruning scheme is implemented in order to successfully identify the two modes of interest. For a given partial of frequency f_n, the components that are "too weak" in amplitude, "too far" from f_n, that are over-damped, or diverging, are discarded. Then, within the poles that passed this first sorting stage, simple physical considerations are used to identify potential pairs of components: the damping factor for component 2 (associated to $\vec{y}$ when there is no coupling) will be lower than that of component 1 (associated to $\vec{z}$). The final choice of the pair of components is done based on "how well" each pair models the partial (using the Reconstruction Signal to Noise Ratio, a.k.a. RSNR).

5 Results

In order to validate the approach presented in Sec. 3, we conducted a few tests on synthetic signals. They all have the same fundamental frequency: 110 Hz, so the signals generated simulate plucks on the open Vth string, assuming standard tuning.

The first synthetic signal considered is the impulse response of a system with transfer function:

$$\mathcal{T}(z) = \frac{\mathcal{P}}{1 - \mathcal{A}z^{-D}} + \frac{\mathcal{Q}}{1 - \mathcal{B}z^{-D}}$$

where $\mathcal{A}$, and $\mathcal{B}$ are computed from Eq. (6) and Eq. (7), using constant values for $\mathcal{H}_l$, $\mathcal{H}_y$, $\mathcal{H}_z$, and $\mathcal{H}_c$. The effect of the plucking position was not included while the values of $\mathcal{Q}$ and $\mathcal{P}$ were found based on Eq. (4) and Eq. (5). Several signals were generated using values of θ_r spanning from 0 ° to 90 °. These signals were analyzed using the analysis framework of Sec. 4. A value of the estimated angle of release was computed for all partials under study (20 in this example) using the exact coefficients from Eq. (22). The median value of those estimates was taken as the final estimate. The circles in Fig. 4 represent the values of $\hat{\theta}_r$ versus the actual value, θ_r, along the dashed line. We see that the trend of θ_r is well estimated despite a constant bias of the estimate: $\hat{\theta}_r$ tends to be slightly bigger than θ_r. The mean absolute error is $\simeq 6.5$ °.

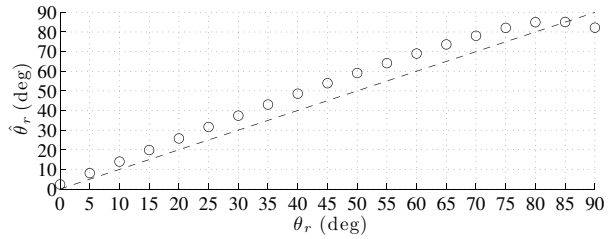

Figure 4: Estimated vs. real value of θ_r, for a synthetic signal of fundamental frequency 110 Hz, with $\mathcal{H}_y = 0.985, \mathcal{H}_z = 0.98, \mathcal{H}_l = -0.999, \mathcal{H}_c = 0.015$.

A second test was done including the effect of the plucking position. The transfer functions used were therefore of the form:

$$\mathcal{T}(z) = \frac{\mathcal{P}\mathcal{V}_{ex}}{1 - \mathcal{A}z^{-D}} + \frac{\mathcal{Q}\mathcal{V}_{ex}}{1 - \mathcal{B}z^{-D}}$$

The relative plucking position was set to $R = 0.15$. This means that the comb filter due to the plucking position in Eq. (2) had a delay $2\mathcal{M} = (1 - R)F_s/f_0$, where F_s is the sampling rate in Hz. The rest of the parameters were the same as in the previous experiment. The results of the estimation of θ_r are shown in Fig. 5. The results are similar to those obtained previously: the trend of the variation of the angle is well extracted. The mean absolute error is now of the order of $\simeq 1.6$ °. The slightly more important drift towards 90 ° is most likely due to the fact that $\tan(\theta_r)$ diverges for this value of θ_r.

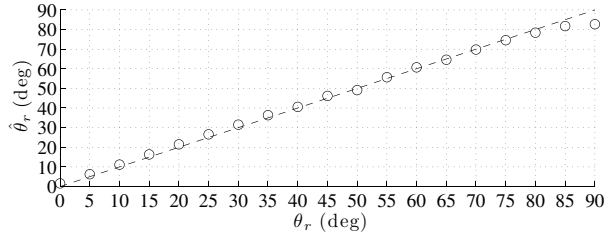

Figure 5: Estimated vs. real value of θ_r, for a synthetic signal, including the effect of the plucking position. The parameters are the same as in Fig. 4.

Another test we performed consisted in using the the DW model presented in Sec. 2 with constant values for the reflectances. The results can be seen in Fig. 6. The estimation

is good for all angles except in 40 °, where the two components are not separated by ESPRIT (there is only one pole with frequency 110 Hz). Without that value, the average absolute error is of 1.9 °.

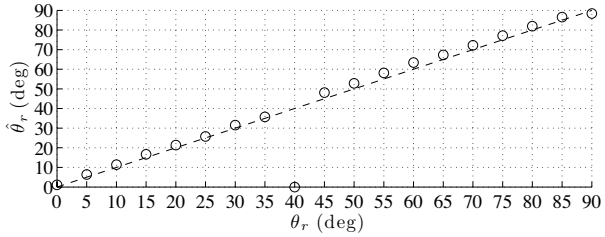

Figure 6: Estimated vs. actual values of θ_r, for a synthetic signal generated using the complete DW model, with with $\mathcal{H}_y = 0.985, \mathcal{H}_z = 0.98, \mathcal{H}_l = -0.999, \mathcal{H}_c = 0.015$.

The tests performed on simple signal models yielded estimates of θ_r that were coherent with the target values. A bias was observed in all cases, although it was much more prominent for the simple model than for the more realistic signals used in the second and third tests. In any cases, the cause for this bias needs to be identified. It may be due to errors in the estimation of the ratio, $\hat{g}_{1k}/\hat{g}_{2k}$. This conclusion was drawn after we observed that the estimates of $\mathcal{A}_k$, $\mathcal{B}_k$ and $\mathcal{H}_{lk}$ were very good (of the order of 1 % in magnitude).

6 Conclusion

This paper has discussed the first tests of a method for the extraction of θ_r, the angle with which a classical guitar string has been released, from the analysis of velocity measurements at the bridge. The physical model of a string underlying our approach was presented in Sec. 2. The formal expression of θ_r as a function of parameters that can be estimated from velocity measurements was derived in Sec. 3. In Sec. 4, the analysis framework used to extract those signal parameters was outlined. Finally, in Sec. 5, we presented and discussed the first results we obtain for the estimation of θ_r for synthetic signals. Future work will focus on improving the quality of the estimation for synthetic signals of increasing likeness with real sounds.The analysis of real velocity signals will then be undertaken.

References

[1] M. Aramaki, J. Bensa, L. Daudet, P. Guillemain, and R. Kronland-Martinet. Resynthesis of coupled piano string vibrations based on physical modeling. *J. New Music Research*, 30(3):213–226, 2001.

[2] B. Bank and M. Karjalainen. Passive admittance matrix modeling for guitar synthesis. In *Proc. of the 13th Int. Conference on Digital Audio Effects (DAFx-10)*, Graz, Austria, 2010.

[3] L. Daudet, P. Guillemain, and R. Kronland-Martinet. Resynthesis of piano strings vibrations based on physical modeling. In *Proc. Int. Comp. Mus. Conf.*, pages 48–51, 1999.

[4] T. J. W. Hill, B. E. Richardson, and S. J. Richardson. Acoustical parameters for the characterisation of the classical guitar. *Acustica – Acta Acustica*, 90(2):335–38, 2004.

[5] J. Laroche. The use of the matrix pencil method for the spectrum analysis of musical signals. *J. Acoust. Soc. Am.*, 4:1958–65, 1993.

[6] H.-M. Lehtonen, V. Välimäki, and T. I. Laasko. Canceling and selecting partials from musical tones using fractional-delay filters. *Computer Music Journal*, 32(2):43–56, Summer 2008.

[7] M. Pavlidou. *A Physical Model of the String-Finger Interaction on the Classical Guitar*. PhD thesis, University of Wales, Cardiff, 1997.

[8] R. Roy, A. Paulraj, and T. Kailath. ESPRIT – a subspace rotation approach to estimation of parameters of cisoids in noise. *IEEE Trans. on Acoustics, Speech, Signal Processing*, 34(5):1340–2, October 1986.

[9] J. Schneider. *The contemporary guitar*, volume 5 of *New Instrumentation*. University of California Press, Berkeley, 1985.

[10] J. O. Smith. *Physical Audio Signal Processing*. Online Book, 2011.

[11] J. O. Smith and X. Serra. PARSHL: An analysis/synthesis program for nonharmonic sounds based on sinusoidal representation. In *Proc. Int. Comp. Mus. Conf.*, 1987.

[12] J. Taylor. *Tone Production on the Classical Guitar*. Musical New Services Ltd., 1978.

[13] C. Traube and P. Depalle. Deriving the plucking point along a guitar string from a least-square estimation of a comb filter delay. In *Proc. of IEEE CCECE*, pages 2001–3, May 2003.

[14] J. Woodhouse. Plucked guitar transients: Comparison of measurements and synthesis. *Acustica – Acta Acustica*, 90:945–65, 2004.